Angiogenesis (2012) 15:59–70
DOI 10.1007/s10456-011-9243-z

ORIGINAL PAPER

Foretinib demonstrates anti-tumor activity and improves overall survival in preclinical models of hepatocellular carcinoma

Hung Huynh · Richard Ong · Khee Chee Soo

Received: 19 September 2011 / Accepted: 8 December 2011 / Published online: 21 December 2011

Abstract
Purpose of study Hepatocellular carcinoma (HCC) is the third leading cause of cancer death. Although sorafenib has been shown to improve survival of patients with advanced HCC, this improvement is modest and patients eventually have refractory disease. The purpose of this study is to assess the anti-tumor and anti-angiogenic activities of foretinib, a vascular endothelial growth factor receptor 2 (VEGFR-2) and c-Met inhibitor using mouse models of human HCC.
Experimental techniques SK-HEP1 and 21-0208 HCC cells as well as patient-derived HCC models were employed to study the anti-tumor and antiangiogenic activities of foretinib. Changes of biomarkers relevant to hepatocyte growth factor (HGF) signaling pathways were determined by Western blotting. Microvessel density, apoptosis and cell proliferation were analyzed by immunohistochemistry.
Results Treatment of SK-HEP1 cells with foretinib resulted in growth inhibition, G2/M cell cycle arrest, reduced colony formation and blockade of HGF-induced cell migration. In both orthotopic and ectopic models of HCC, foretinib potently inhibited tumor growth in a dose-dependent manner. Inhibition of angiogenesis correlated with inactivation of VEGFR-2/c-Met signaling pathways. Foretinib also caused elevation of p27 and Bim but reduced cyclin B1 expression and p–c-Myc, which resulted in a reduction in cellular proliferation and the induction of tumor cell apoptosis. In an orthotopic model, foretinib potently inhibited primary tumor growth and significantly prolonged mouse survival.
Data interpretations Foretinib demonstrated significant antitumor activities in patient-derived HCC xenograft models. This study provides a compelling rationale for clinical investigation in patients with advanced HCC.

Keywords Foretinib · HCC · Growth inhibition · Angiogenesis

Introduction

With an annual incidence of over 660,000 deaths, HCC is the fifth most common malignancy and the third leading cause of cancer-related mortality globally [1]. Despite the available treatment options, the incidence still nearly equals to the mortality rate. More than 80% of patients with HCC have inoperable disease with very poor prognosis [2]. Therefore, potentially curative treatment like locoregional ablation, surgical resection or liver transplantation can be achieved only in a minority of HCC patients [3]. Even in resectable HCC, 5-year-survival rates only range between 15 and 39% [4], largely due to recurrent disease. As such, there is clearly a need for effective novel therapies to combat this deadly disease. Meta-analysis evaluating 37 chemotherapy randomized clinical trials demonstrated almost complete lack of efficacy for HCC [3, 5]. Sorafenib has been shown to improve the median survival of HCC patients from 7.9 to 10.7 months [6]. Although the availability of sorafenib is likely to have a considerable clinical impact, there remains a need for additional treatment

Electronic supplementary material The online version of this article (doi:10.1007/s10456-011-9243-z) contains supplementary material, which is available to authorized users.

H. Huynh (✉) · R. Ong · K. C. Soo
Laboratory of Molecular Endocrinology, Division of Molecular and Cellular Research, National Cancer Centre, 11 Hospital Drive, Singapore 169610, Singapore
e-mail: cmrhth@nccs.com.sg

options for patients with advanced HCC. This unmet need may be met in the future by one or more of the novel inhibitors currently in the development.

HCC tumors are highly vascular and VEGF is one of the factors regulating this process. The VEGFR–2 is expressed on endothelial cells and activation of VEGFR-2 by VEGF plays a primary role in tumor angiogenesis and survival signals to these cells [7]. Elevated VEGF is associated with poor prognosis, early recurrence and short time survival in HCC [8, 9]. Like VEGFR-2, hepatocyte growth factor (HGF) and c-Met have been implicated in HCC [10, 11]. Point mutations in c-*MET* have been identified in HCC [12]. c-Met overexpression is seen in 20–48% of HCC tumors [13–16] and has been associated with decreased 5-year survival [14]. Simultaneous administration of HGF and VEGF in cultured primary endothelial cells confers a greater proliferative stimulus and pro-angiogenic effect than either ligand alone, suggesting a co-operation between c-Met and VEGFR-2 in endothelial cells [17]. Expression of c-Met is regulated by the same hypoxia-inducible factor system that governs VEGF expression levels; hence, both c-Met and VEGF are induced in response to tumor hypoxia [18]. Recent biomarker data from a phase III sorafenib study identified elevated HGF levels as a potential predictor of poor prognosis in HCC [19]. These findings suggest that simultaneous inhibition of c-Met and VEGFR-2 by a small-molecule inhibitor may confer broad and potent anti-tumor efficacy.

Foretinib (XL880, GSK1363089) is a small-molecule kinase inhibitor that targets members of the HGF and VEGF receptor tyrosine kinase families, with additional inhibitory activity toward AXL, c-Kit, Flt-3, PDGF-Rβ, and Tie-2 [20, 21]. Foretinib inhibited cellular HGF-induced c-Met phosphorylation and VEGF-induced extracellular signal-regulated kinase phosphorylation and prevented both HGF-induced responses of tumor cells and HGF/VEGF-induced responses of endothelial cells [21]. In vivo, a single 100 mg/kg oral gavage dose of foretinib resulted in substantial inhibition of HGF/VEGF–induced phosphorylation of c-Met in liver and VEGFR-2 in lung through 24 h [21]. Collectively, these data indicate that foretinib may prevent tumor growth through a direct effect on tumor cell proliferation and by inhibition of invasion and angiogenesis mediated by HGF and VEGF [21]. A recent phase I study using foretinib in solid tumors found the maximally tolerated dose to be 240 mg/day [22]. Preliminary analysis revealed that partial response was observed in two patients with papillary RCC and one patient with medullary thyroid carcinoma [22]. Minimal changes were detected in total c-Met and total RON; however, kinase activity as measured by phosphorylation status, as well as the downstream signaling molecules p-Akt and p-ERK, was reduced in the tumors of three patients. In addition, marked decreases in proliferation and increases in apoptosis in the tumor biopsies were observed post treatment [22]. A phase I/II, open-label, multicenter study of foretinib in adult subjects with HCC is ongoing (NCT00920192).

Here, we report the results of a study assessing the effects of foretinib on tumor growth and angiogenesis in xenograft models of human HCC which have been previously established and characterized to evaluate new agents for treatment of HCC [23].

Materials and methods

Reagents

Research grade Capsitol was purchased from CyDex, Inc., Lenexa, Kansas, USA. Antibodies against Akt, Bim, Bad, Ship1, Gab1, PLC-γ1, cleaved PARP and phosphorylation-specific antibodies against c-Met Tyr1234/1235, c-Met Tyr1003, PLC-γ1 Tyr1253, ERK1/2 Thr202/Tyr204, Histone 3 Ser10, c-Myc Thr58/Ser62, cdk-2 Thr14/Tyr15 and c-Raf were obtained from Cell Signaling Technology, Beverly, MA. The antibodies against phospho-PDGF-Rβ Tyr1021, phospho-VEGFR-2 Tyr951, PDGF-Rβ, VEGFR-2, c-Met, cyclin B1, cdk-2, cdk-4, cdk-6, p27 and α-tubulin were from Santa Cruz Biotechnology Inc, Santa Cruz, CA. CD31/platelet endothelial cell adhesion molecule 1 antibody were was from BioLegend, San Diego, CA, USA.. The chemiluminescent detection system was supplied by Amersham, Pharmacia Biotech, Arlington Heights, IL.

Cell culture

21-0208 HCC cells were isolated from 21-0208 tumors as described previously [24]. Human hepatoma SK-HEP1 (HTB-52) cells were obtained from American Type Culture Collection (Manassas, VA, USA). They were maintained as monolayer cultures in Hi-Gluc-DMEM (DMEM) supplemented with 10% fetal bovine serum (FBS) and 1% penicillin–streptomycin (growth medium) at 37°C, 5% CO_2.

To determine the effects of foretinib on cell number, SK-HEP1 cells were plated at a density of 2×10^4 cells per dish and treated with various concentrations of foretinib ranging from 0.25 to 1.5 μM in DMEM containing 1% FBS for 48 h. Cell number was determined manually with a hemocytometer. The data were expressed as mean ± SE.

Flow cytometry analysis

SK-HEP1 cells were plated at the density of 5×10^5 and then treated with either 0.1% DMSO or indicated doses

(0, 0.25, 0.5, 1, and 1.5 μM) of foretinib for 24 h. Cells were fixed in 70% ethanol at 4°C for 24 h and stained with propidium iodide. Fluorescence intensity of the stained cells was measured using FACSCalibur flow cytometer (BD, San Jose, CA). Data were analyzed using BD CellQuest Pro software. For every measurement, 10,000 events were collected, and gating was set to exclude cell doublets. DNA contents of certain phases were shown as percentage compared to the total DNA content within the gate.

Colony formation assay

10×10^2 SK-HEP1 cells were suspended in growth medium in the absence or presence of 1 μM of foretinib. Cells were seeded in triplicate into 100 × 20 mm cell culture dishes (Greiner Bio-One GmbH, Frickenhausen, Germany) and allowed to grow for 10 days. Colonies were visualized by staining the cells with 0.5% crystal violet and pictures were captured using Nikon E8400 camera.

Wound-healing scratch assay

SK-HEP1 cell monolayer grown to confluence on 100 mm culture dishes were wounded by scratching with a pipette tip. They were briefly washed with serum free DMEM and cultured in the presence of 1 μM foretinib or 50 ng/ml human recombinant hepatocyte growth factor (HGF) or the combination of foretinib and HGF for 24 h. The wounds were photographed (10× objective) at 24 h. Each experiment was done in triplicate.

Efficacy of foretinib on the tumor growth of ectopic and orthotopic models of HCC

This study received ethics board approval at the National Cancer Centre of Singapore and Singapore General Hospital. All mice were maintained according to the *Guide for the Care and Use of Laboratory Animals* published by the National Institutes of Health, USA.

Foretinib (GSK1363089G, free base, micronized) was from GlaxoSmithKline, Collegeville, PA, USA. It was diluted either in 30% Capsitol (Capsitol in water) or 1% Hydroxypropyl methylcellulose: 0.2% Sodium Lauryl Sulfate: 98.8% water at an appropriate concentration prior use. HCC tumors have previously been used to create xenograft lines [23], of which the following lines (06-0606, 5-1318, 26-1004, and 21-0208) were used to establish tumors in male *SCID* mice (Animal Resources Centre, Canning Vale, Western Australia) aged 9–10 weeks. The 5-1318 and 06-0606 xenografts were derived from Hepatitis B virus positive HCC while 26-1004 had wild type p53 and 16 bp deletion in exon 8 of *PTEN* gene. 5-1318 had mutation in codon 249 of *p53* gene.

For dose response experiments, mice bearing 06-0606 or 5-1318 tumors were administered indicated doses of foretinib for indicated times. 6 mg/kg and 10 mg/kg doses were given daily while 30 mg/kg dose was administered every other day. Each treatment group is comprised of 10–14 animals. Treatment started when the tumors reached the size of approximately 100–200 mm^3. Tumor growth was monitored and tumor volume was calculated as described [23]. At the end of the study, the mice were sacrificed with body and tumor weights recorded and the tumors harvested for analysis.

21-0208, 06-0606 and 26-1004 orthotopic models of HCC were created as previously described [24]. Mice bearing tumors were administered vehicle and 3 doses of foretinib: 6 mg/kg (daily), 10 mg/kg (daily) and 30 mg/kg (every other day) for indicated days. Each treatment group is comprised of 10–14 animals. Treatments started on day 9. By this time, the tumors reached the size of approximately 100–150 mm^3. Tumor-bearing mice were sacrificed when control mice became moribund and tumor volume recorded.

For time-dependent effects of foretinib, mice bearing 06-0606 tumors were randomized (12 mice/group) and daily treated with vehicle or 30 mg/kg foretinib. Tumors were collected daily for 4 days after dosing (2 animals per time point) for analysis.

To determine the extent of hypoxia in tumor tissues, mice bearing 06-0606 tumors were treated with vehicle (30% Captisol), or foretinib (15 mg/kg) or bevacizumab (10 mg/kg) or sorafenib (20 mg/kg) for 14 days. Mice were i.p. injected with pimonidazole hydrochloride (60 mg/kg, 2.5 μl/g of mouse body weight) 1 h before tumors harvested. Hypoxic regions of tumor were identified by staining the sections with Hypoxyprobe plus Kit HP2 (Chemicon) as described by the manufacturer.

Survival study

Mice bearing orthotopic 06-0606 tumors were daily received either vehicle (1% Hydroxypropyl methylcellulose: 0.2% Sodium Lauryl Sulfate: 98.8% Water) or 15 mg/kg foretinib for 18 days. Each treatment group is comprised of 10 animals. Body weight, ascites formation, and overall survival were monitored daily. Tumor-bearing mice were sacrificed when they became moribund, and the presence of ascitic fluid was recorded for each mouse. The size of primary orthotopic tumors was also recorded.

Immunohistochemistry

For cleaved PARP and p-Histone 3 Ser10 stainings, tumor samples were processed for paraffin embedding. For CD31 staining, they were embedded in Optimal Cutting

Temperature (Sakura Finetek Inc., Torrance, CA, USA). 5-μm sections were stained with anti-CD31, anti-p-Histone 3 Ser10 and anti-cleaved PARP antibodies to assess microvessel density, cell proliferation, and apoptosis, respectively, as described [24]. The number of p-Histone 3 Ser10 and cleaved PARP positive cells among at least 500 cells per region was counted and expressed as percentage values. For the quantification of mean micro-vessel density in sections stained for CD31, 10 random fields at a magnification of ×100 were captured for each tumor.

Western blot analysis

To determine the changes in indicated proteins, 3–4 independent tumors from vehicle and foretinib-treated mice were homogenized separately in lysis buffer as described previously [23]. Eighty μg of proteins per sample were analyzed by Western blot analysis as described [23]. Blots were incubated with indicated primary antibodies and horseradish peroxidase-conjugated secondary antibodies. All primary antibodies were then visualized with chemiluminescent detection system (Amersham, Pharmacia Biotech).

Statistical analysis

For quantification analysis, the sum of the density of bands corresponding to protein blotting with the antibody under study was calculated and normalized with α-tubulin. After normalization, changes in the expression of the protein under study in treated samples were expressed relative to the basal levels of this protein in vehicle treated sample. Comparisons of tumor growth over time were performed using ANOVA followed by Student's t-test. Body weight and tumor burden of mice at the point of sacrifice, differences in the levels of protein under study, tumor weight at sacrifice, p-Histone 3 Ser10 index, mean microvessel density, and cleaved PARP-positive cells were compared

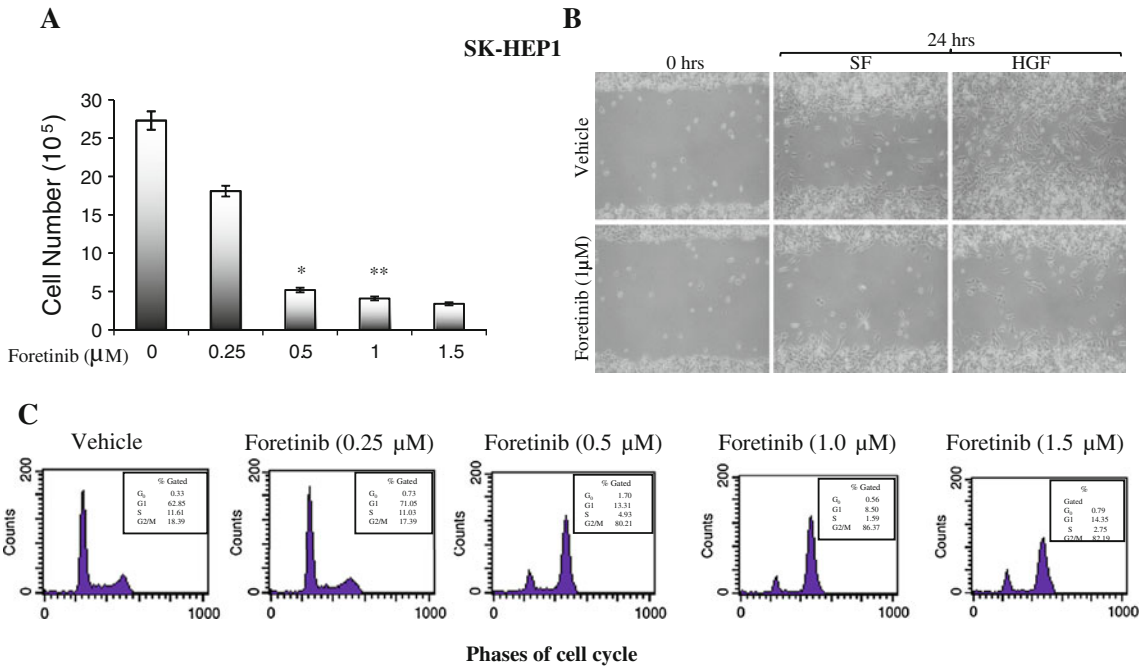

Phases of cell cycle

Foretinib (μM)	G_0	G_1	S	G_2/M
0	0.33 ± 0.2	62.8 ± 4*	11.6 ± 2.5*	18.4 ± 2.6*
0.25	0.73 ± 0.3	70.3 ±4*	11.03 ± 1.8*	17.4 ± 2.3*
0.5	1.3 ± 0.4	13.3 ± 26**	4.9 ± 1.2**	80.1 ± 5**
1.0	0.56 ± 0.3	8.5 ± 2.1**	3.4 ± 0.6***	86.4 ± 3.2**
1.5	0.6 ± 0.3	0.4 ± 3.1**	2 ± 0.8***	85.1 ± 2.9**

Fig. 1 Effects of foretinib on the proliferation, cell cycle progression and cell motility of SK-HEP1 cells. Cells were plated and treated with indicated concentrations of foretinib in DMEM containing 1% FBS for 24 h as described in "Materials and methods". Cell number (**a**), cell motility assay (**b**) and cell cycle analysis and quantification of cells in different phases of cell cycle (**c**) in the presence and absence of foretinib are shown. *Different asterisks* indicate significantly different from one another at $P < 0.05$. Experiments were repeated at least twice

using Student's t test. For survival study, Log-rank test was used. For statistical analysis, significance was established at $P < 0.05$.

Results

Because c-Met transduces multiple biological activities, including motility, proliferation, survival and metastasis [25, 26], we evaluated the in vitro activity of foretinib using SK-HEP1 cells. Figure 1a shows that treatment of SK-HEP1 cells with 0.25, 05, 1 and 1.5 μM foretinib resulted in 30, 60, 68 and 70% reduction in cell number, respectively when analyzed on day 2. Maximal inhibition was observed at approximately 1 μM. Foretinib also blocked HGF-induced cell motility (Fig. 1b) and caused G_2/M phase arrest with reduction in the G_0/G_1 and S phases (Fig. 1c). The number of colony in the vehicle-and foretinib-treated cells at 2 μM was 873 ± 81 and 63 ± 20 respectively, suggesting that foretinib significantly inhibits colony formation ($P < 0.05$). In 21-0208 HCC cells, foretinib inhibited phosphorylation of c-Met, Gab1, VEGFR-2, PDGFR-β, Akt and ERK1/2 and induced apoptosis (Fig. 1S, supplementary data).

We next tested the antitumor activity of foretinib in vivo. For dose response curve, treatment began when mean tumor volume was 100–200 mm^3. As shown in Fig. 2, the growth rate of 06-0606 xenografts was decreased by foretinib in a dose-dependent manner ($P < 0.05$). Oral administration of foretinib at 6 mg/kg (once daily), 10 mg/kg (once daily) and 30 mg/kg (once every other day) resulted in 46, 68 and 83% tumor growth inhibition, respectively when analyzed on day 16. The effects of foretinib are relatively rapid, showing significant difference in tumor volume in the treated group within 8 days ($P < 0.05$); however, tumor regression was not observed (Fig. 2b). Similarly, treatment of 5-1318 tumor-bearing mice with 15 mg/kg (daily) and 30 mg/kg foretinib (once every other day) for 14 days resulted in approximately 53 and 87% reductions in tumor burden respectively (Fig. 2S, supplementary data). No overt toxicity, as defined by weight loss (Fig. 2a), unkempt appearance, mortality and behavior, was observed in any foretinib groups during the course of treatment. The dose between 15 and 20 mg/kg/day was deemed efficacious with no observed drug-associated toxicities.

Immunohistochemical analysis revealed that c-Met expression was detected both in endothelial cells and cancer cells but VEGFR-2 expression was found only on endothelial cells (Fig. 3S, supplementary data). These are consistent with previous observations [27]. Treatment with

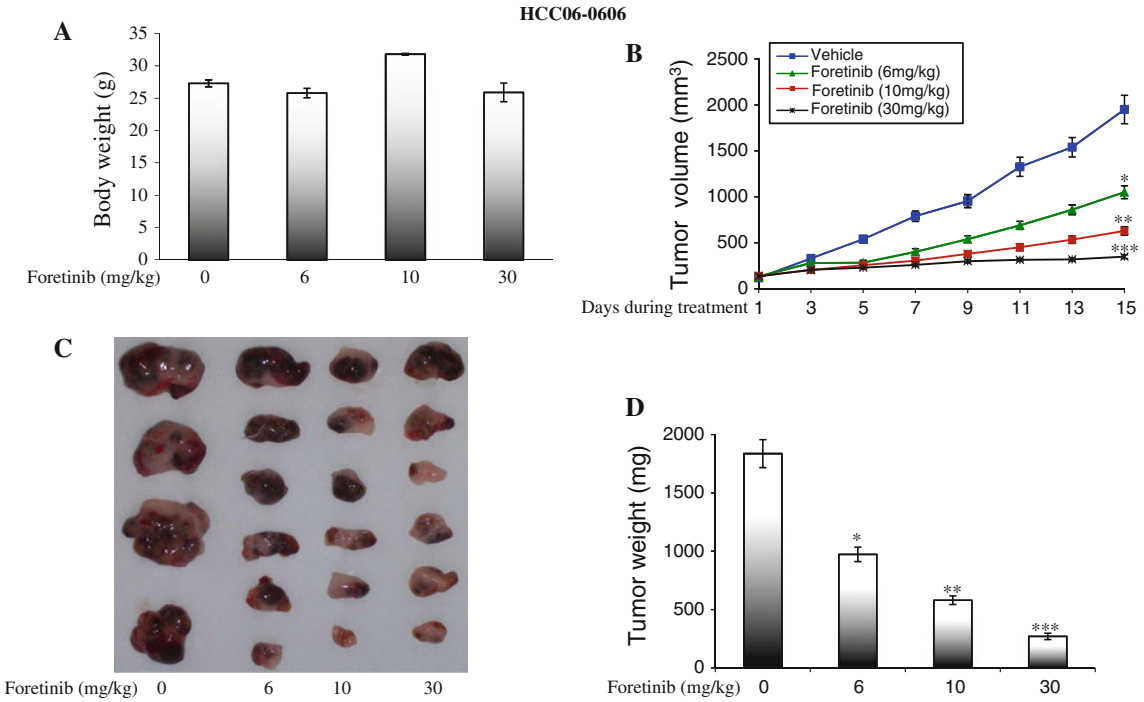

Fig. 2 Dose-dependent effects of foretinib on tumor growth of patient-derived xenograft line 06-0606. 06-0606 tumors were s.c implanted in *SCID* mice as described in "Materials and methods". Mice bearing tumors were treated with vehicle (30% Captisol) or 3 doses of foretinib (6 and 10 mg/kg daily and 30 mg/kg every other day) for 15 days as described in "Materials and methods". Each treatment arm involved 14 independent tumor-bearing mice. Mean of body weight at sacrifice (**a**), tumor volume ± SE at given time points (**b**), representative vehicle- and foretinib-treated tumors (**c**) and the corresponding tumor weight (**d**) for 06-0606 xenografts are shown. *Different asterisks* indicate significantly different from one another at $P < 0.05$. Experiments were repeated twice with similar results

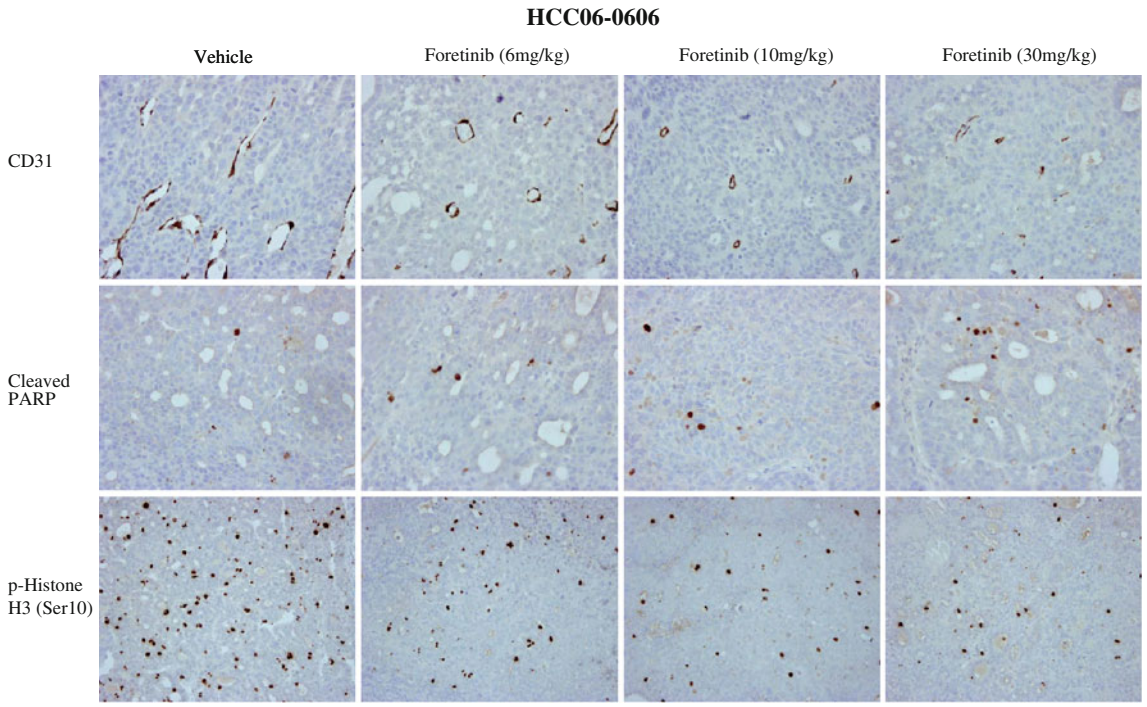

Fig. 3 Dose-dependent effects of foretinib therapy on angiogenesis, cell proliferation and apoptosis in 06-0606 xenograft. Mice bearing tumor xenografts were treated with vehicle (30% Captisol) or 3 doses of foretinib: 6 and 10 (daily) and 30 mg/kg (every other day) for 15 days as described in Fig. 2. Each treatment arm involved 14 independent tumor-bearing mice. Representative pictures of blood vessels stained with anti-CD31, proliferative cells stained with p-Histone 3 Ser10, and apoptotic cells stained with anti-cleaved-PARP antibodies in vehicle- and foretinib-treated tumors are shown (200×). Experiments were repeated twice with similar results

foretinib led to dose-dependent decrease in blood microvessel density, which is consistent with inhibition of angiogenesis (Fig. 3). The mean microvessel density in the tumors that were treated with vehicle and foretinib at 6 mg/kg, 10 mg/kg and 30 mg/kg (once every other day) was approximately 12.4 ± 2.4., 6.2 ± 2.1, 4.2 ± 0.6 and 2.2 ± 0.3, respectively. The differences in blood microvessel density between control and 10 mg/kg foretinib and between 10 mg and 30 mg/kg foretinib were statistically significant ($P < 0.05$). The percentage of p-Histone Ser10 labeling cells in the tumors that were treated with vehicle and foretinib at 6 mg/kg, 10 mg/kg and 30 mg/kg (once every other day) were approximately 14.6 ± 1.7, 7.2 ± 1.8, 3.2 ± 0.9 and 2.3 ± 0.5%, respectively. The differences in p-Histone positive cells in vehicle- and foretinib-treated tumors were statistically significant ($P < 0.05$). In addition, the percentage of cleaved PARP positive cells in the control and foretinib at 6 mg/kg, 10 mg/kg and 30 mg/kg (once every other day) was approximately 0.4 ± 0.1, 0.6 ± 0.3, 0.7 ± 0.3 and 3.8 ± 0.5%, respectively. The differences in cleaved PARP-positive cells in vehicle and 30 mg/kg foretinib-treated tumors were statistically significant ($P < 0.05$). Micrographs of 06-0606 tumors stained for pimonidazole (hypoxia) showed that the amount and distribution of hypoxia increased after foretinib, bevacizumab and sorafenib treatments (Fig. 4S, supplementary data).

We investigated the potential mechanisms of foretinib in 06-0606 tumors. As expected, the levels of p-VEGFR-2 Tyr951 and p–c-Met at Tyr1234/1235 were significantly decreased by foretinib therapy in a dose-dependent manner (Fig. 4a, $P < 0.05$). The levels of p-ERK1/2, p-PLCγ1 and p-Akt in tumors treated with either 15 mg or 30 mg/kg foretinib were significantly reduced ($P < 0.05$). Since altered expressions of cell cycle regulators and apoptotic proteins have been implicated in cellular proliferation and cell death and clinical outcome of HCC, we investigated the expressions of key genes involved in the cell cycle. As shown in Fig. 4b, foretinib treatment led to a significant decrease in cyclin B1 and p–c-Myc ($P < 0.05$) but caused a significant elevation of Bim, cleaved PARP and p27 ($P < 0.05$). There were no significant alterations in the levels of cdk-6, cdk-2, p–cdk-2 and cdk-4 by foretinib therapy. The data suggest that foretinib inhibited cell proliferation and caused cell death.

We next examined the time-dependent effects of foretinib on phosphorylation of c-Met and VEGFR-2. First, daily dose of 30 mg/kg was administered 06-0606 tumor-bearing mice, then tumors were collected daily for 4 days and lysates prepared from two tumor-bearing mice per time

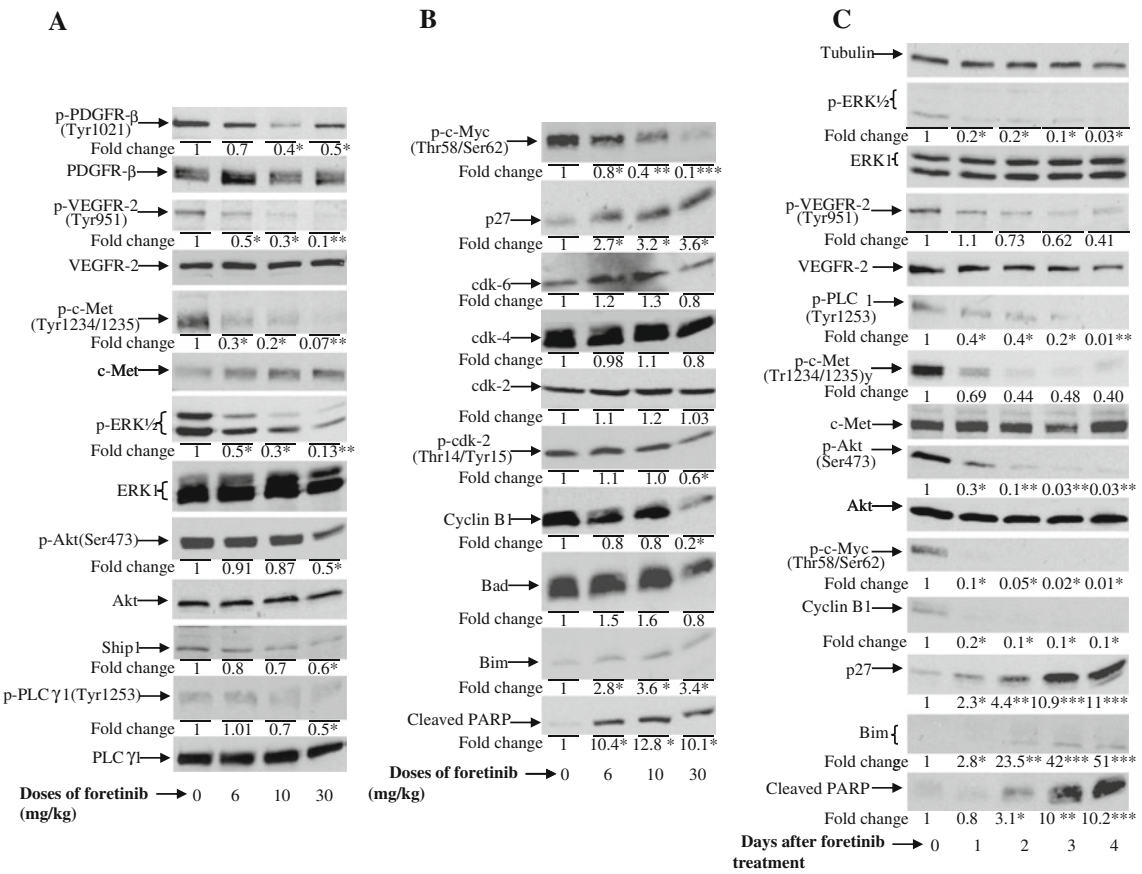

Fig. 4 Dose-dependent and time-dependent effects of foretinib on the activation of VEGFR-2, PDGF-Rβ, c-Met, Akt and ERK1/2, expression of cell cycle regulatory proteins and apoptosis in HCC xenograft line 06-0606. 06-0606 tumors were s.c implanted in *SCID* mice as described in Fig. 1. Mice bearing tumor xenografts were treated with vehicle (30% Captisol) or 3 doses of Foretinib: 6 and 10 mg/kg (daily) and 30 mg/kg (every other day) for 15 days (**a**, **b**). For time-dependent effect of foretinib, mice bearing tumors were daily given 30 mg/kg foretinib and tumors were collected daily for 4 days (**c**). Each treatment arm involved 14 independent tumor-bearing mice. Lysates from vehicle- and foretinib-treated tumors were subjected to Western blotting described in "Materials and methods". Blots were incubated with the indicated antibodies. Representative Western blots and quantification analysis (expressed as fold of controls) are shown. *Different asterisks* indicate significantly different from one another at $P < 0.05$. Experiments were repeated at least twice with similar results

point were analyzed. Figure 4c showed that foretinib blocked the autophosphorylation of VEGFR-2 and c-Met in a time-dependent manner. As PLCγ1, ERK and Akt signaling pathways are downstream of VEGFR-2 and c-Met, we investigated whether these pathways were altered in foretinib-treated tumors. There was a significant decrease in p-ERK, p-Akt, and p-PLCγ1 within 24 h of foretinib treatment (Fig. 4c, $P < 0.05$), suggesting that the VEGFR-2/c-Met pathways were inhibited. While the levels of cyclin B1 and p–c-Myc in foretinib-treated samples were significantly reduced ($P < 0.05$), the 89 kDa cleaved PARP fragment and Bim were readily detected in foretinib but not in vehicle-treated samples. Notably, upregulation of Bim coincided with the appearance of the apoptotic marker, cleaved PARP, indicating that foretinib induced apoptosis.

To test the antitumor activity of foretinib in a specific organ environment, an orthotopic model was used. In this model, tumor fragments were implanted into the liver of *SCID* mice. In 26-1004, 21-0208 and 06-0606 models of HCC, all mice developed tumors with the size of approximately 100–150 mm^3 within 8–10 days of tumor implantation. Figure 5 showed that the growth of tumor xenograft was inhibited by foretinib as determined by tumor volume at the end of treatment. In 06-0606 xenograft, foretinib produced a dose-dependent reduction of tumor volume by 30 ± 5, 62 ± 7 and 83 ± 6% with doses of 6, 15 and 30 mg/kg, respectively (Fig. 5). Similarly, foretinib treatment led to a dose-dependent decrease in primary tumor growth of 68 ± 8 and 89 ± 5% (for 26-1004 line) and 75 ± 7 and 91 ± 5% (for 21-0208 line) at 15 and 30 mg/kg doses, respectively. The differences in tumor volume between vehicle- and foretinib-treated tumors were statistically significant ($P < 0.05$). The results demonstrate the ability of foretinib to block the

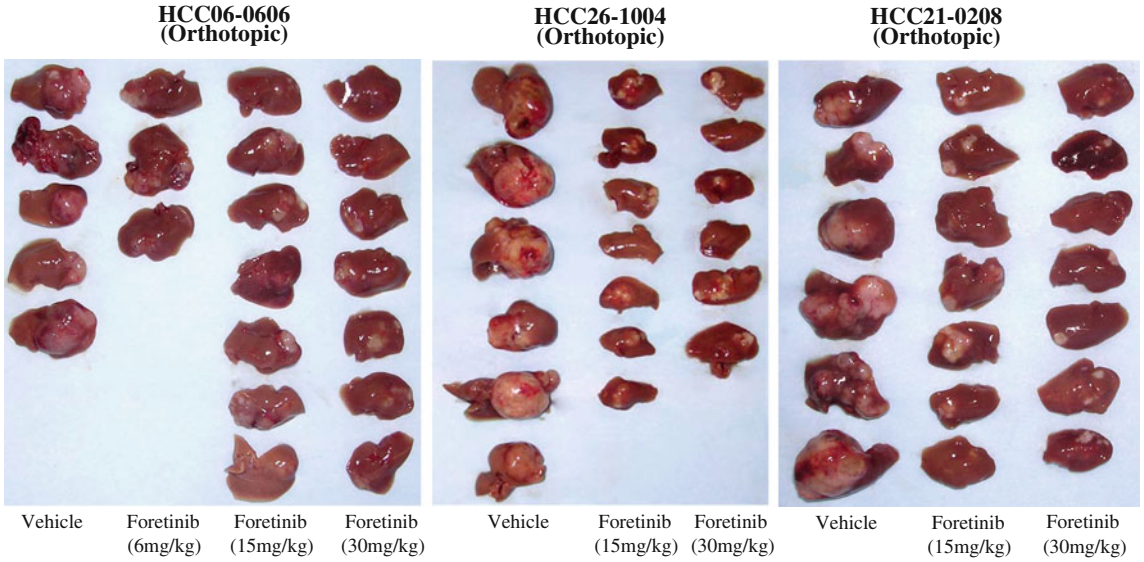

Fig. 5 Dose-dependent effects of foretinib on the growth of orthotopic HCC xenografts. Indicated tumors were implanted in the livers of *SCID* mice as described in "Materials and methods". Mice bearing tumor xenografts were treated with vehicle (30% Captisol) or indicated doses of foretinib for 18 days as described in "Materials and methods". Each treatment arm involved 10–14 independent tumor-bearing mice. Treatments started on day 9. By this time, the tumors reached the size of approximately 100–150 mm^3. Representative vehicle- and foretinib-treated 06-0606, 26-1004 and 21-0208 tumors are shown. Experiments were repeated twice with similar results

tumor growth in an organ environment. This study also provided an indication of the tolerability of foretinib as the treated groups had no significant reduction in body weight.

Next, we evaluated the effect of the foretinib therapy on HCC proliferation, angiogenesis and apoptosis in 26-1004 orthotopic model. Figure 6 showed that foretinib significantly decreased in CD31-positive cells, confirming that foretinib inhibits angiogenesis. The mean microvessel density in the tumors that were treated with vehicle and foretinib at 15 and 30 mg/kg (once every other day) was approximately 16.2 ± 3.4., 1.2 ± 0.4, and 0.8 ± 0.3, respectively. The differences in blood microvessel density between control and foretinib treatment were statistically significant ($P < 0.05$). The percentage of p-Histone Ser10 labeling cells in the tumors that treated orally with vehicle and foretinib at 15 mg/kg (daily) and 30 mg/kg (once every other day) were approximately 10.3 ± 2.2, 3.2 ± 0.4, and 2.9 ± 0.5 respectively confirming that foretinib inhibits cell proliferation. Additionally, a significant elevation in cleaved PARP positive cells was seen in foretinib-treated tumors, suggesting that foretinib induces apoptosis. The percentage of cleaved PARP positive cells in the control and foretinib at 15 and 30 mg/kg (once every other day) was approximately 0.3 ± 0.1, 2.8 ± 0.5, and $4.6 \pm 0.9\%$, respectively. The differences in cleaved PARP- positive cells in vehicle- and foretinib-treated tumors were statistically significant ($P < 0.05$). Similar data were obtained when 21-0208 and 06-0606 tumors were analyzed (data not shown).

Finally, we tested if foretinib might confer a therapeutic benefit in these animals, initiating treatment 9 days after tumor inoculation. As expected, vehicle-treated mice developed a swollen abdomen, indicative of ascites formation, and became highly cachetic within 4 weeks of tumor introduction. Upon autopsy, the abdomens of injected mice exhibited large volumes of ascites (2–4 ml), and large tumors grown in the liver. Foretinib treatment potently inhibited the tumor growth and small sized tumors were detectable in treated livers. A Kaplan–Meier survival analysis confirmed that while all mice in the vehicle-treated group were moribund at days 45, the foretinib-treated mice had a significantly prolonged overall survival and 80% mice were still alive at the day 75 ($P < 0.01$, log-rank test, Fig. 7).

In conclusion, the results of the current study show that molecular targeting of AXL, VEGFR-2 and c-Met by foretinib inhibited the growth of HCC xenografts and significantly prolonged mouse survival. This may represent an alternative strategy in the treatment of HCC.

Discussion

HCC is the third leading cause of cancer-related mortality globally [1]. The number of deaths per year in HCC is virtually identical to the incidence, illustrating the high case mortality rate of this aggressive disease [1]. While the use of sorafenib heralded a major breakthrough in HCC

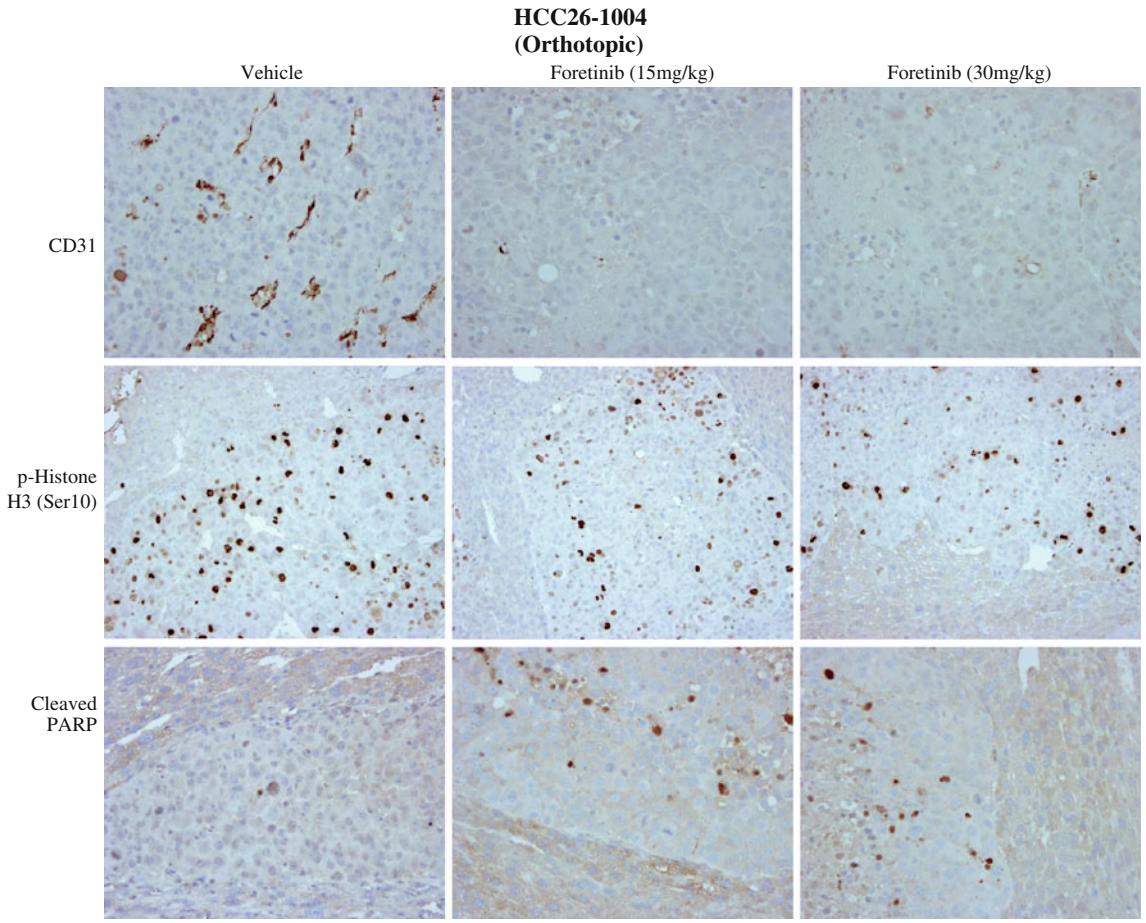

Fig. 6 Effects of foretinib and on angiogenesis, cell proliferation and apoptosis of orthotopic 26-1004 xenograft. 26-1004 tumors were implanted in the liver of *SCID* mice as described in Fig. 5. Mice bearing tumors were treated indicated dose of foretinib for 18 days. Representative pictures of blood vessels stained with anti-CD31, proliferative cells stained with anti-phospho-histone 3 Ser10, and apoptotic cells stained with anti-cleaved-PARP antibodies in vehicle- and drug-treated tumors are shown (200×). Experiments were repeated twice with similar results

cancer therapy, the benefit is at best modest and confers a rather transient clinical benefit [6, 28]. Therefore, additional treatment options are warranted. In the present study, we investigated the antitumor and antiangiogenic activities of foretinib, which targets VEGFR-2 and c-Met signaling pathways. We employed both ectopic and orthotopic models of human HCC, which recapitulate many features of human HCC [23, 24, 29]. Considerable antitumor activity was demonstrated in both ectopic and orthotopic models of when foretinib was given at a dose of 15 mg/kg/day or 30 mg (every other day). In an orthotopic model of HCC, foretinib potently inhibited primary tumor growth and significantly prolonged survival of mice. Foretinib decreased c-Met and VEGFR-2 phosphorylation, and reduced downstream signaling of p-ERK and p-Akt in treated tumors with an increase in cleaved PARP. Reduction in tumor cell proliferation, induction of tumor hypoxia and apoptosis in combination with the antiangiogenic effect of foretinib may result in significant antitumor efficacy. Our findings are consistent with the recent study by You et al., [30] who reported that in the Rip1Tag2 mouse model of pancreatic islet cancer, treatment with foretinib resulted in inhibition of tumor vasculature, widespread intratumoral hypoxia and tumor cell apoptosis.

The precise molecular mechanisms responsible for antitumor effects of foretinib remain to be elucidated. In eukaryotic cells, entry into mitosis is controlled by the activation of the cyclin B/Cdc-2 protein kinase, resulting in degradation of cyclin B. In this study, we observed that foretinib treatment caused elevation of p27 and reduction in cyclin B1, suggesting that foretinib may cause G2/M cell cycle arrest. Indeed, treatment of SK-HEP1 cells with foretinib resulted in G2/M cell cycle arrest. It has been shown that over-expression of c-Myc induced HCC [31–33], whereas inhibition of c-Myc expression resulted in the differentiation of tumor cells and eventually most of the cells underwent death [34]. In the present study, we showed by Western blot analysis that treatment with

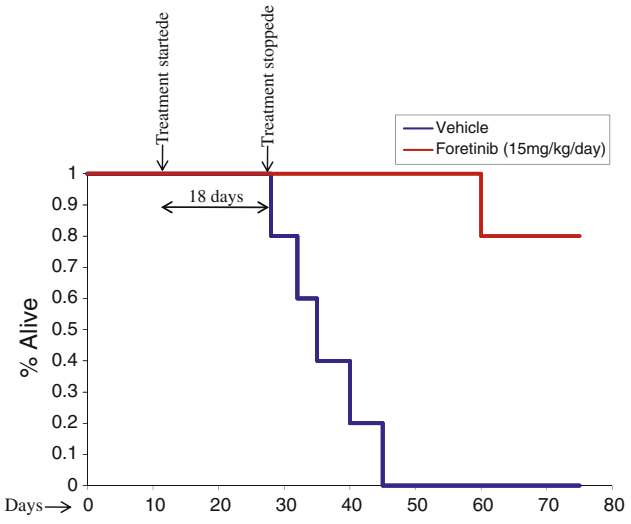

Fig. 7 Therapeutic effects of foretinib on tumor burden and survival of mice bearing 06-0606 orthotopic tumors. 06-0606 tumors were implanted in the livers of male *SCID* mice as described under "Materials and methods". Upon tumor establishment (day 9 after tumor implantation), mice (10 per group) were randomized and daily treated with either vehicle (0.2 ml of 1% Hydroxypropyl methylcellulose: 0.2% Sodium Lauryl Sulfate: 98.8% Water) or 15 mg/kg/day foretinib for 18 days as described in "Materials and methods". Tumor-bearing mice were sacrificed when they became moribund. Kaplan–Meier survival analysis was shown. While all mice in the vehicle-treated groups were moribund at day 45, mice treated with foretinib exhibited significantly prolonged overall survival ($P < 0.01$, log-rank test). 80% of mice in foretinib-treated group were still alive at day 75

foretinib led to the decrease in p–c-Myc Thr58/Ser62 in a dose-dependent manner. Upregulation of Bim coupled with reduction in p-c-Myc may be in part responsible for the observed apoptosis in foretinib-treated tumors. Inhibition of angiogenesis (through inactivation of VEGFR-2 and c-Met on stroma and endothelium) was demonstrated by a reduction in microvessel density in tumor xenografts after administration of foretinib. Direct inhibition of HGF activation on tumor cells was confirmed by an inhibition of HGF-induced SK-HEP1 cell motility and colony formation in vitro and a reduction in phosphorylation of these receptors as well as signaling pathway components (ERK and PLCγ1) in 21-0208 HCC cells and tumor xenografts (Fig. 4). The above data indicate that the effects of foretinib appear to be a result of its dual mechanisms of action: antiangiogenesis and direct antitumor activity.

The degree to which inhibition of the c-Met signaling pathway contributes to antiangiogenesis and anti-proliferation and how much of these effects are contributed by inhibition of other foretinib targets, such as AXL, VEGFR-2, PDGF-Rβ, and Tie-2 [20, 21] remain to be determined. It has been reported that AXL stimulation by GAS6 results in inhibition the VEGF activation of VEGFR-2 [35]. In the 06-0606 and 21-0208 HCC tumor models, AXL expression was low (data not shown). It remains to determine whether the inhibition of VEGFR-2 activity on endothelial cells as the results of direct inhibition of AXL or AXL stimulation through GAS6 as reported in other models [35]. In the present study, SK-HEP1 cells responded to HGF and all HCC xenografts tested express detectable levels of c-Met. These observations suggest potential HGF-driven autocrine/paracrine growth pathways exist. Inhibition of HGF-induced SK-HEP1 cell motility and greater anti-tumor activity seen in foretinib-treated mice could also plausibly be explained by the ability of foretinib to inhibit c-Met signaling pathway that is implicated in the pathogenesis of HCC [12]. Recent evidence implicates upregulation of HGF and c-Met after VEGF-inhibitory therapies as a mechanism of resistance to angiogenesis inhibitors [36, 37]. Moreover, expression of both VEGFR-2 and c-Met is upregulated as a result of tumor hypoxia, and these receptors cooperate to increase tumor cell invasiveness and drive angiogenesis [18]. Additionally, both c-Met and VEGFR-2 upregulate expression of VEGF regulated genes, preventing endothelial apoptosis, promoting capillary formation in vivo and increasing the microvessel density in tumors [17, 38]. These observations raise the possibility that c-Met signaling pathway in concert with VEGFR-2, plays an important role in growth and metastasis of cancer cells and activation of the c-Met signaling pathway during VEGF-targeted antiangiogenic therapy as a result of elevation of HGF and c-Met may contribute in part to the observed increased tumor invasiveness and metastasis [39–41].

It has been reported that point mutations in c-Met have been identified in HCC [12]. c-Met over-expression is seen in 20–48% of HCC tumors [13–16] and is associated with decreased 5-year survival [14]. Up-regulation of both VEGF and Met occurs in tumor cells under hypoxic conditions, and VEGF signaling synergizes with HGF to promote tumor growth, angiogenesis, and invasion [18]. Thus, dual inhibition of c-Met and VEGF receptors may inhibit growth and survival mechanisms activated by tumor cells in response to hypoxic stress and may be particularly effective in addressing the most lethal aspects of tumor growth, such as migration, invasion, and metastasis. The realization that foretinib effectively inhibits VEGFR-2, c-Met, angiogenesis and primary tumor growth and produces survival benefit, has clinical implications. This is being explored in a phase I, dose-escalation trial of oral foretinib. Although the clinical efficacy of foretinib has yet to be determined, preliminary analysis of phase I study showed some biological activity and clinical efficacy. Several studies with c-Met- and HGF-specific antibodies or small molecular inhibitors of c-Met are ongoing [42].

In conclusion, the results of the current study show that molecular targeting of c-Met/VEGFR-2 by foretinib

inhibited primary tumor growth and significantly prolonged mouse survival. This could represent an alternative strategy in the treatment of HCC.

Acknowledgments We would like to thank GSK for foretinib. This work was supported by grants from National Medical Research Council of Singapore, Singapore Millennium Foundation, Singapore Cancer Syndicate (SCS-AS0032, SCS-HS0021, SCS-AMS0086) to Huynh Hung.

References

1. Jemal A, Siegel R, Xu J, Ward E (2010) Cancer statistics, 2010. CA Cancer J Clin 60:277–300
2. Okuda K, Ohtsuki T, Obata H, Tomimatsu M, Okazaki N, Hasegawa H, Nakajima Y, Ohnishi K (1985) Natural history of hepatocellular carcinoma and prognosis in relation to treatment. Study of 850 patients. Cancer 56:918–928
3. Llovet JM, Burroughs A, Bruix J (2003) Hepatocellular carcinoma. Lancet 362:1907–1917
4. Takenaka K, Kawahara N, Yamamoto K, Kajiyama K, Maeda T, Itasaka H, Shirabe K, Nishizaki T, Yanaga K, Sugimachi K (1996) Results of 280 liver resections for hepatocellular carcinoma. Arch Surg 131:71–76
5. Farazi PA, DePinho RA (2006) Hepatocellular carcinoma pathogenesis: from genes to environment. Nat Rev Cancer 6:674–687
6. Llovet JM, Ricci S, Mazzaferro V, Hilgard P, Gane E, Blanc JF, de Oliveira AC, Santoro A, Raoul JL, Forner A, Schwartz M, Porta C, Zeuzem S, Bolondi L, Greten TF, Galle PR, Seitz JF, Borbath I, Haussinger D, Giannaris T, Shan M, Moscovici M, Voliotis D, Bruix J (2008) Sorafenib in advanced hepatocellular carcinoma. N Engl J Med 359:378–390
7. Hicklin DJ, Ellis LM (2005) Role of the vascular endothelial growth factor pathway in tumor growth and angiogenesis. J Clin Oncol 23:1011–1027
8. Poon RT, Ho JW, Tong CS, Lau C, Ng IO, Fan ST (2004) Prognostic significance of serum vascular endothelial growth factor and endostatin in patients with hepatocellular carcinoma. Br J Surg 91:1354–1360
9. Chao Y, Li CP, Chau GY, Chen CP, King KL, Lui WY, Yen SH, Chang FY, Chan WK, Lee SD (2003) Prognostic significance of vascular endothelial growth factor, basic fibroblast growth factor, and angiogenin in patients with resectable hepatocellular carcinoma after surgery. Ann Surg Oncol 10:355–362
10. Kaposi-Novak P, Lee JS, Gomez-Quiroz L, Coulouarn C, Factor VM, Thorgeirsson SS (2006) Met-regulated expression signature defines a subset of human hepatocellular carcinomas with poor prognosis and aggressive phenotype. J Clin Invest 116:1582–1595
11. Osada S, Kanematsu M, Imai H, Goshima S (2008) Clinical significance of serum HGF and c-Met expression in tumor tissue for evaluation of properties and treatment of hepatocellular carcinoma. Hepatogastroenterology 55:544–549
12. Park WS, Dong SM, Kim SY, Na EY, Shin MS, Pi JH, Kim BJ, Bae JH, Hong YK, Lee KS, Lee SH, Yoo NJ, Jang JJ, Pack S, Zhuang Z, Schmidt L, Zbar B, Lee JY (1999) Somatic mutations in the kinase domain of the Met/hepatocyte growth factor receptor gene in childhood hepatocellular carcinomas. Cancer Res 59:307–310
13. Boix L, Rosa JL, Ventura F, Castells A, Bruix J, Rodes J, Bartrons R (1994) c-met mRNA overexpression in human hepatocellular carcinoma. Hepatology 19:88–91
14. Ueki T, Fujimoto J, Suzuki T, Yamamoto H, Okamoto E (1997) Expression of hepatocyte growth factor and its receptor, the c-met proto-oncogene, in hepatocellular carcinoma. Hepatology 25:619–623
15. Suzuki K, Hayashi N, Yamada Y, Yoshihara H, Miyamoto Y, Ito Y, Ito T, Katayama K, Sasaki Y, Ito A (1994) Expression of the c-met protooncogene in human hepatocellular carcinoma. Hepatology 20:1231–1236
16. Kiss A, Wang NJ, Xie JP, Thorgeirsson SS (1997) Analysis of transforming growth factor (TGF)-alpha/epidermal growth factor receptor, hepatocyte growth Factor/c-met, TGF-beta receptor type II, and p53 expression in human hepatocellular carcinomas. Clin Cancer Res 3:1059–1066
17. Xin X, Yang S, Ingle G, Zlot C, Rangell L, Kowalski J, Schwall R, Ferrara N, Gerritsen ME (2001) Hepatocyte growth factor enhances vascular endothelial growth factor-induced angiogenesis in vitro and in vivo. Am J Pathol 158:1111–1120
18. Pennacchietti S, Michieli P, Galluzzo M, Mazzone M, Giordano S, Comoglio PM (2003) Hypoxia promotes invasive growth by transcriptional activation of the met protooncogene. Cancer Cell 3:347–361
19. Pena C, Shan M, Wilhelm S, Lathia C (2008) Hepatocyte growth factor (HGF) is a prognostic biomarker for overall survival and a pharmacodynamic biomarker for sorafenib response in the SHARP phase III HCC trial. 33rd European society for medical oncology (ESMO) congress, Sept 12–16, 2008, Stockholm, Sweden. Abstract #4600
20. Liu L, Greger J, Shi H, Liu Y, Greshock J, Annan R, Halsey W, Sathe GM, Martin AM, Gilmer TM (2009) Novel mechanism of lapatinib resistance in HER2-positive breast tumor cells: activation of AXL. Cancer Res 69:6871–6878
21. Qian F, Engst S, Yamaguchi K, Yu P, Won KA, Mock L, Lou T, Tan J, Li C, Tam D, Lougheed J, Yakes FM, Bentzien F, Xu W, Zaks T, Wooster R, Greshock J, Joly AH (2009) Inhibition of tumor cell growth, invasion, and metastasis by EXEL-2880 (XL880, GSK1363089), a novel inhibitor of HGF and VEGF receptor tyrosine kinases. Cancer Res 69:8009–8016
22. Eder JP, Shapiro GI, Appleman LJ, Zhu AX, Miles D, Keer H, Cancilla B, Chu F, Hitchcock-Bryan S, Sherman L, McCallum S, Heath EI, Boerner SA, LoRusso PM (2010) A phase I study of foretinib, a multi-targeted inhibitor of c-Met and vascular endothelial growth factor receptor 2. Clin Cancer Res 16:3507–3516
23. Huynh H, Soo KC, Chow PK, Panasci L, Tran E (2006) Xenografts of human hepatocellular carcinoma: a useful model for testing drugs. Clin Cancer Res 12:4306–4314
24. Huynh H, Ngo VC, Koong HN, Poon D, Choo SP, Toh HC, Thng CH, Chow P, Ong HS, Chung A, Goh BC, Smith PD, Soo KC (2010) AZD6244 enhances the antitumor activity of sorafenib in ectopic and orthotopic models of human hepatocellular carcinoma (HCC). J Hepatol 52:79–87
25. Birchmeier C, Birchmeier W, Gherardi E, Vande Woude GF (2003) Met, metastasis, motility and more. Natl Rev Mol Cell Biol 4(12):915–925
26. Rosario M, Birchmeier W (2003) How to make tubes: signaling by the Met receptor tyrosine kinase. Trends Cell Biol 13:328–335
27. Bussolino F, Di Renzo MF, Ziche M, Bocchietto E, Olivero M, Naldini L, Gaudino G, Tamagnone L, Coffer A, Comoglio PM (1992) Hepatocyte growth factor is a potent angiogenic factor which stimulates endothelial cell motility and growth. J Cell Biol 119:629–641
28. Cheng AL, Kang YK, Chen Z, Tsao CJ, Qin S, Kim JS, Luo R, Feng J, Ye S, Yang TS, Xu J, Sun Y, Liang H, Liu J, Wang J, Tak WY, Pan H, Burock K, Zou J, Voliotis D, Guan Z (2009) Efficacy and safety of sorafenib in patients in the Asia-Pacific region with advanced hepatocellular carcinoma: a phase III randomised, double-blind, placebo-controlled trial. Lancet Oncol 10:25–34

29. Huynh H, Ngo VC, Fargnoli J, Ayers M, Soo KC, Koong HN, Thng CH, Ong HS, Chung A, Chow P, Pollock P, Byron S, Tran E (2008) Brivanib alaninate, a dual inhibitor of vascular endothelial growth factor receptor and fibroblast growth factor receptor tyrosine kinases, induces growth inhibition in mouse models of human hepatocellular carcinoma. Clin Cancer Res 14:6146–6153
30. You WK, Sennino B, Williamson CW, Falcón B, Hashizume H, Yao LC, Aftab DT, McDonald DM (2011) VEGF and c-Met blockade amplify angiogenesis inhibition in pancreatic islet cancer. Cancer Res 71(14):4758–4768
31. Sandgren EP, Quaife CJ, Pinkert CA, Palmiter RD, Brinster RL (1989) Oncogene-induced liver neoplasia in transgenic mice. Oncogene 4:715–724
32. Murakami H, Sanderson ND, Nagy P, Marino PA, Merlino G, Thorgeirsson SS (1993) Transgenic mouse model for synergistic effects of nuclear oncogenes and growth factors in tumorigenesis: interaction of c-myc and transforming growth factor alpha in hepatic oncogenesis. Cancer Res 53:1719–1723
33. Wu Y, Renard CA, Apiou F, Huerre M, Tiollais P, Dutrillaux B, Buendia MA (2002) Recurrent allelic deletions at mouse chromosomes 4 and 14 in Myc-induced liver tumors. Oncogene 21:1518–1526
34. Shachaf CM, Kopelman AM, Arvanitis C, Karlsson A, Beer S, Mandl S, Bachmann MH, Borowsky AD, Ruebner B, Cardiff RD, Yang Q, Bishop JM, Contag CH, Felsher DW (2004) MYC inactivation uncovers pluripotent differentiation and tumour dormancy in hepatocellular cancer. Nature 431:1112–1117
35. Gallicchio M, Mitola S, Valdembri D, Fantozzi R, Varnum B, Avanzi GC, Bussolino F (2005) Inhibition of vascular endothelial growth factor receptor 2-mediated endothelial cell activation by Axl tyrosine kinase receptor. Blood 105(5):1970–1976
36. Sennino B, Naylor RM, Tabruyn SP, You WK, Aftab DA, McDonald DM (2009) Reduction of tumor invasiveness and metastasis and prolongation of survival of RIP-Tag2 mice after inhibition of VEGFR plus c-Met by XL184. Mol Cancer Ther 8:A13
37. Shojaei F, Lee JH, Simmons BH, Wong A, Esparza CO, Plumlee PA, Feng J, Stewart AE, Hu-Lowe DD, Christensen JG (2010) HGF/c-Met acts as an alternative angiogenic pathway in sunitinib-resistant tumors. Cancer Res 70:10090–10100
38. Zhang YW, Su Y, Volpert OV, Vande Woude GF (2003) Hepatocyte growth factor/scatter factor mediates angiogenesis through positive VEGF and negative thrombospondin 1 regulation. Proc Natl Acad Sci USA 100:12718–12723
39. Loges S, Mazzone M, Hohensinner P, Carmeliet P (2009) Silencing or fueling metastasis with VEGF inhibitors: antiangiogenesis revisited. Cancer Cell 15:167–170
40. Ebos JM, Lee CR, Cruz-Munoz W, Bjarnason GA, Christensen JG, Kerbel RS (2009) Accelerated metastasis after short-term treatment with a potent inhibitor of tumor angiogenesis. Cancer Cell 15:232–239
41. Paez-Ribes M, Allen E, Hudock J, Takeda T, Okuyama H, Vinals F, Inoue M, Bergers G, Hanahan D, Casanovas O (2009) Antiangiogenic therapy elicits malignant progression of tumors to increased local invasion and distant metastasis. Cancer Cell 15:220–231
42. Comoglio PM, Giordano S, Trusolino L (2008) Drug development of MET inhibitors: targeting oncogene addiction and expedience. Nat Rev Drug Discov 7:504–516